AAPS PharmSciTech, Vol. 15, No. 4, August 2014 (© 2014)
DOI: 10.1208/s12249-014-0139-2

Research Article

Theme: Translational Application of Nano Delivery Systems: Emerging Cancer Therapy
Guest Editors: Mahavir B. Chougule and Chalet Tan

Encapsulation in Nanoparticles Improves Anti-cancer Efficacy of Carboplatin

Tanmoy Sadhukha[1] and Swayam Prabha[1,2,3]

Received 3 December 2013; accepted 24 April 2014; published online 16 May 2014

Abstract. Poor cellular uptake contributes to high dose requirement and limited therapeutic efficacy of the platinum-based anticancer drug carboplatin. Delivery systems that can improve the cellular accumulation of carboplatin will, therefore, likely improve its therapeutic potential. The objective of this study was to evaluate nanoparticles composed of the biodegradable polymer, poly(D, L-lactide-*co*-glycolide), for carboplatin delivery to tumor cells. Carboplatin-loaded nanoparticles were formulated by double emulsion-solvent evaporation technique. Nanoparticles demonstrated sustained release of carboplatin over 7 days. Cellular uptake of carboplatin encapsulated in nanoparticles was several fold higher than that with free carboplatin in A549 (lung) and MA148 (ovarian) tumor cells. *In vitro* cytotoxicity studies showed that encapsulation of carboplatin in nanoparticles resulted in a remarkable reduction in the IC_{50} of carboplatin in several cell lines (up to 280-fold in some cells). Confocal microscopic analysis revealed the presence of carboplatin nanoparticles in several cellular compartments including lysosomes, cytoplasm, and the nucleus. These results demonstrate an enhanced cellular uptake of carboplatin through encapsulation in PLGA nanoparticles and suggest that improved therapeutic efficacy and reduced toxicity may be achieved with this approach.

KEY WORDS: carboplatin; cell uptake; chemotherapy; cytotoxicity; nanoparticles.

INTRODUCTION

Platinum-based drugs, carboplatin and cisplatin, are used in the treatment of a number of malignancies including ovarian, lung, head, and neck cancers (1–3). While carboplatin is often preferred over cisplatin due to the lower incidence of nephrotoxicity and ototoxicity, the former is significantly less potent and is still associated with the risk of cumulative toxicities (4, 5). Low uptake of carboplatin by tumor cells is considered a key reason for its limited therapeutic efficacy (6). This is evident by the need of administration of a large number of doses in multiple cycles (beyond six cycles) to achieve tumor inhibition (7).

Several attempts have been made to increase the effectiveness of platinum compounds and thereby reduce the number of required dosing cycles (8–12). Recent studies (13, 14) with liposomes containing platinum drugs demonstrated the potential of these carriers to improve the cytotoxicity in several cancer cell lines. It was suggested that increased intracellular accumulation of liposome-encapsulated drugs results in higher cytotoxicity. Although effective in killing cells, liposomes suffer from poor stability in plasma, which results in rapid release of the drug before reaching the target site (15). Hence, a more effective delivery system is needed to improve the therapeutic efficacy of platinum-based drugs.

In this study, nanoparticles composed of poly(D-L-lactide-*co*-glycolide) (PLGA) polymer were prepared as a means to produce safe and effective carriers for carboplatin (16–18). Because of their small size, nanoparticles are effectively endocytosed by tumor cells, which results in high cellular uptake of the encapsulated payload (19). We hypothesized that encapsulation of carboplatin in PLGA nanoparticles would significantly increase the delivery of carboplatin into tumor cells and thereby result in improved anticancer efficacy. To test this hypothesis, carboplatin-loaded PLGA nanoparticles were fabricated, and their cytotoxicity and uptake were evaluated in a panel of cancer cell lines.

MATERIALS AND METHODS

Materials

Carboplatin, polyvinyl alcohol (PVA), and chloroform were purchased from Sigma (St. Louis, MO). Penicillin/streptomycin, fetal bovine serum, RPMI 1640, Dulbecco's phosphate buffered saline (DPBS), trypsin-EDTA solution, LysoTracker red, DAPI, and wheat germ agglutinin (Texas red) were obtained from Invitrogen Corporation (Carlsbad, CA). Ester-terminated 50:50 poly(D-L-lactide-*co*-glycolide)

[1] Department of Pharmaceutics, College of Pharmacy, University of Minnesota, Minneapolis, Minnesota 55455, USA.
[2] Center for Translational Drug Delivery, University of Minnesota, Minneapolis, Minnesota 55455, USA.
[3] To whom correspondence should be addressed. (e-mail: prabh025@umn.edu)

 1530-9932/14/0400-1029/0 © 2014 American Association of Pharmaceutical Scientists

(inherent viscosity: 0.95–1.2 dl/g) was purchased from Lactel Absorbable Polymers (Birmingham, AL).

Methods

Formulation of Carboplatin Loaded Nanoparticles

Carboplatin and the green fluorescent probe, coumarin-6, were loaded into PLGA nanoparticles by a modification of the previously reported double emulsion-solvent evaporation technique (17). In an attempt to increase the loading efficiency of the carboplatin in nanoparticles, two different approaches were evaluated.

In the first method (Method A), 3 mg of carboplatin was dissolved in 300 μl of 2.5% *w/v* PVA to form the innermost aqueous phase. The carboplatin solution was emulsified into the organic phase (32 mg PLGA and 250 μg coumarin-6 in 1 ml chloroform) by sonicating at 10 W for 45 s (Model W-375, Heat Systems Ultrasonics Inc., CT). This W/O emulsion was immediately transferred into 7.5 ml of 2.5% *w/v* PVA and sonicated at 20 W power for 3 min to form the W/O/W emulsion. Chloroform was evaporated by stirring overnight under ambient conditions followed by 1 h stirring under vacuum. In the second method (Method B), the innermost aqueous phase comprised of 3 mg carboplatin dissolved in 300 μl of 1% *w/v* bovine serum albumin solution. Following emulsification of the carboplatin solution in the organic phase (as in Method A), the W/O emulsion was transferred to 7.5 ml of 2.5% *w/v* PVA and sonicated at 20 W power for 3 min. Chloroform was evaporated using a rotary evaporator for 1 h. In both cases, the resulting nanoparticle dispersion was washed three times by ultracentrifugation at 148,000*g* for 35 min, and the wash solutions were saved for the analysis of unencapsulated carboplatin. After the final wash, nanoparticles were suspended in purified water and centrifuged at 1,000*g* for 6 min. The supernatant was lyophilized (Labconco, FreeZone 4.5, Kansas City, MO). Control nanoparticles containing coumarin-6 but no carboplatin were also synthesized similarly.

Determination of Carboplatin Loading in Nanoparticles

Carboplatin loading in nanoparticles was analyzed by quantifying both the unencapsulated drug in the wash solution and the encapsulated drug. To determine the encapsulated amount, 1.1 mg of nanoparticles was dispersed in 550 μl of methanol and extracted overnight using a rotary extractor. A portion of the methanolic extract was used for quantification of coumarin-6 loading using a fluorescence plate reader (FLx800, BioTek Instruments). The remaining methanol was evaporated under nitrogen, and the drug was dissolved in 500 μl of HPLC mobile phase under sonication in a bath sonicator for 10 min. Quantification of carboplatin was performed by high-performance liquid chromatography (HPLC) using a C18 column (Eclipse Plus 4.6×250 mm, 5 μm, Agilent Technologies) in isocratic mode. The mobile phase consisted of 90% of 20 mM phosphate buffer (pH 6.75) and 10% acetonitrile at a flow rate of 1 ml/min. Carboplatin was quantified by UV detection at 227 nm at a retention time of 2.6 min. Carboplatin in wash solution was analyzed in a similar manner using carboplatin dissolved in wash solution of control nanoparticles for the preparation of the standard curve (20). Carboplatin loading was also confirmed by using inductively coupled plasma mass spectrometry (ICP-MS; see below).

Physical Characterization of Nanoparticles

The hydrodynamic diameter of nanoparticles was determined using dynamic light scattering. About 1 mg of nanoparticles was dispersed in 2 ml of deionized water by sonication in a bath sonicator for 5 min, and the dispersion was subjected to particle size analysis using a Delsa™ Nano C Particle Analyzer (Beckman, Brea, CA). Measurements were performed at 25°C and at a 165° scattering angle. The mean hydrodynamic diameter was calculated based on size distribution by weight, assuming a log-normal distribution. Three individual size measurement runs were performed for each sample, with each run recording 150 size events. Zeta potential of nanoparticles was also determined using the same instrument.

Scanning electron microscopy (SEM) of carboplatin-loaded PLGA nanoparticles was performed using a Hitachi S-4700 cold field emission gun scanning electron microscope. A drop of an aqueous dispersion of PLGA nanoparticles was placed on a Lacey carbon-coated copper grid (300 mesh, Ted Pella Inc. Redding, CA) and allowed to air-dry. The grid was mounted on the SEM stage and sputter coated with platinum and gold-palladium before imaging.

In Vitro Release Studies

Cumulative carboplatin release from nanoparticles was determined as described previously (21) by dispersing 1 mg/ml carboplatin nanoparticles (Method B) in phosphate buffer, maintained at 37°C. Aliquots of the dispersion were withdrawn at 1 h, 2 h, 4 h, 6 h, 10 h, 1 day, 2 days, 3 days, 5 days, and 7 days, and centrifuged at 17,000*g* for 20 min. Volume of the dispersion withdrawn was replaced with fresh buffer. The supernatant was collected, diluted with acetonitrile, and analyzed by HPLC as described above.

Cell Culture Studies

MA148 (ovarian cancer) cells were a kind gift from Dr. Sundaram Ramakrishnan, University of Minnesota. A549 (human lung adenocarcinoma), NCI-ADR/RES (ovarian cancer cells derived from OVCAR-8 cells), and MDA-MB-231 (human mammary adenocarcinoma) cells were obtained from Dr. Jayanth Panyam, University of Minnesota. All cell lines

Table I. Nanoparticle Characterization

	Control NP	Method A	Method B
Hydrodynamic diameter (nm) (mean ± SD), $n=3$	299.6±0.9	311.0±9.2	325.8±6.7
Polydispersity index	0.13	0.14	0.15
Zeta potential (mV) (mean ± SD), $n=3$	−8.5±0.3	−9.9±0.5	−9.6±0.4
Carboplatin loading (μg/mg NP)	–	1.3	3.4
Encapsulation efficiency (%)	–	1.5	3.9

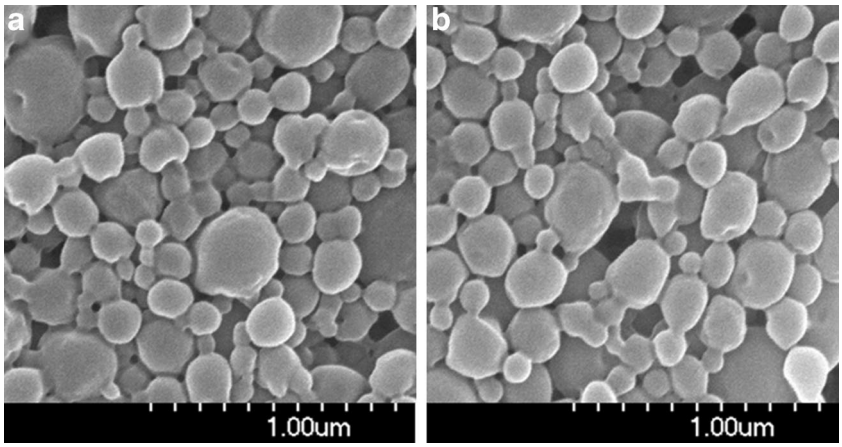

Fig. 1. SEM images of nanoparticles prepared by **a** Method A and **b** Method B. SEM images show similar morphology and size distribution of nanoparticles prepared by the two techniques

were propagated using RPMI 1640 medium supplemented with 10% fetal bovine serum (FBS) and 1% antibiotic solution (final concentration of 100 IU penicillin and 100 μg/ml streptomycin per milliliter of media) and maintained at 37°C and in 5% carbon dioxide.

Cytotoxicity Studies

Cells were plated in 96-well plates at a density of 5,000 cells/well, 1 day prior to treatment addition. Treatment groups included carboplatin-loaded nanoparticles and free carboplatin dissolved in growth medium in concentrations ranging from 1–1,000 μg/ml. Untreated cells and cells treated with control PLGA nanoparticles (containing coumarin-6 but no carboplatin) served as controls. The cells were incubated with the treatment for 1 day following which the cells were washed three times with DPBS and 100 μl of fresh medium was added. MTS assay was performed at designated time intervals following treatment addition. The cell survival profile was fit to a sigmoidal dose response curve using GraphPad Prism software (GraphPad Software, Inc.) to determine the IC_{50} of the drug treatments.

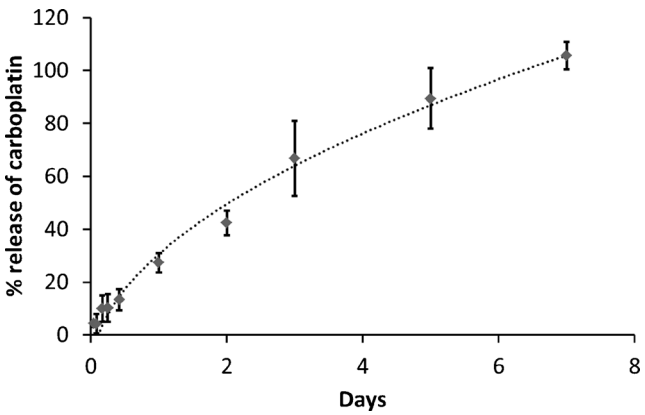

Fig. 2. Carboplatin release from nanoparticles. Carboplatin nanoparticles were dispersed in phosphate buffer and at predetermined times, the dispersion was centrifuged and the supernatant analyzed by HPLC for carboplatin content. Data shown is mean ± SD, $n=3$. *Dotted line* represents Higuchi model fitting of the data

Intracellular Accumulation of Carboplatin

About 1 million A549 and MA148 cells were incubated with 2 μg/ml carboplatin solution or 300 μg/ml carboplatin nanoparticles for 6 h at 37°C. Following incubation, the cells were washed three times with 1 ml of DPBS, 500 μl of sterile water was then added, and the cells were lysed by two freeze-thaw cycles. A part of the cell lysate was used for protein analysis, and the remaining lysate was lyophilized. The lyophilized product was heated at 85°C with 70% nitric acid for 3 h, diluted with water and analyzed for platinum by ICP-MS. A Thermo Scientific XSERIES 2 ICP-MS with ESI PC3 Peltier cooled spray chamber with SC-FAST injection loop and SC-4 autosampler was used. To the diluted samples, 20 ppb of Indium internal standard was added. All the elements were analyzed using He/H_2 collision-reaction mode.

Intracellular Accumulation of Nanoparticles

Uptake of coumarin-6 labeled nanoparticles was evaluated both quantitatively by measuring coumarin-6 concentration and qualitatively by confocal fluorescence microscopy. For quantitative determination, MA148 cells were plated in 96-

Table II. Kinetics and Model Fitting for Carboplatin Release from Nanoparticles

Model	Constraints	Fitting parameters	Slope	R^2
Higuchi	–	F vs. $T^{1/2}$	0.431	0.986
Zero order	Up to 3 days	Q_t vs. T	20.4	0.993
Zero order	–	Q_t vs. T	17.1	0.939
First order	Up to 5 days	Log (Q_t) vs. T	−0.178	0.968
Korsmeyer-Peppas	Less than 60% release	log (F) vs. log (T)	0.632	0.966

Where: F Fraction of Drug Released, T Time, and Q_t Percent Drug Released at Time t

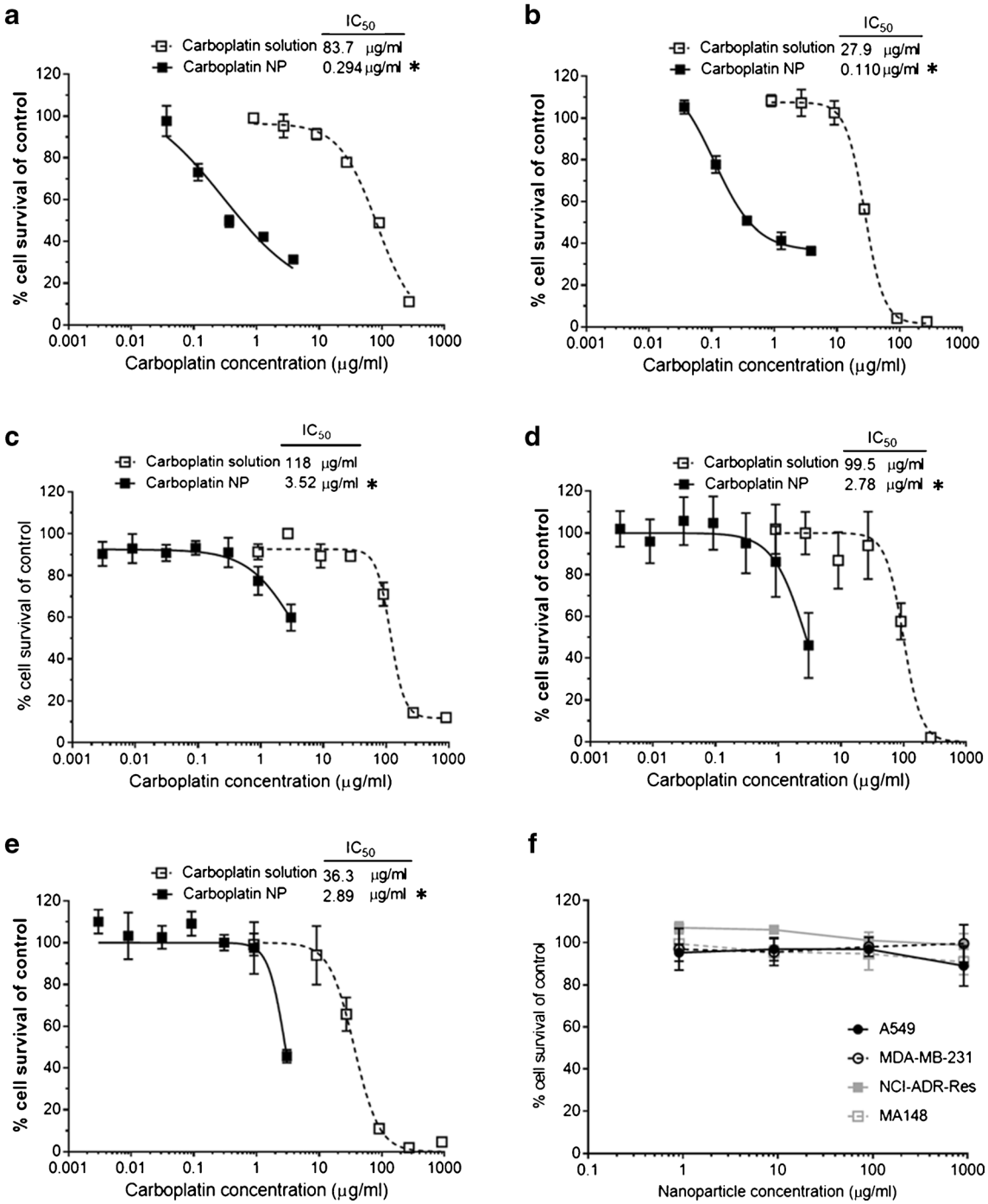

Fig. 3. Enhanced cell kill by carboplatin nanoparticles. MA148, A549, MDA-MB-231, and NCI-ADR/RES were treated with different concentrations of carboplatin in solution or encapsulated in nanoparticles for 3 days. MTS assay was performed each day to determine the percent cell survival using untreated cells as control. Comparison of cell survival as a function of carboplatin concentration and the IC_{50} of the treatments in **a** MA148 after 1 day, **b** MA148 after 2 days, **c** A549 after 2 days, **d** MDA-MB-231 after 3 days, and **e** NCI-ADR/RES after 3 days are plotted. **f** Cells survival after 3 days of treatment with different concentration of control nanoparticles demonstrates lack of toxicity due to nanoparticles themselves. Data shown is mean ± SD, $n=3$. *$P<0.01$

well plates, and 300 μg/ml of nanoparticles were added to the wells and incubated at 37°C for 1, 6, or 24 h. At each time point, cells were washed three times with 1 ml of DPBS and then lysed with 200 μl of RIPA buffer. The cell lysate was centrifuged at 17,000*g* for 10 min, and the supernatant was assayed for protein content using the BCA protein assay kit. To determine the intracellular accumulation of coumarin-6, cell lysates were extracted with methanol for 1 h. The samples were centrifuged, and supernatants were analyzed for coumarin-6 concentration using a fluorescence plate reader (22). The

Table III. IC_{50} of Carboplatin Solution in Cells

	IC_{50} (Mean ± SE) (μg/ml)		
	Day 1	Day 2	Day 3
MA148	83.6±1.4	28.1±1.0	13.7±1.2
NCI-ADR/RES	1753.0±4.4	193.0±1.9	37.4±1.7
A549	776.0±1.9	118.0±1.2	64.3±1.1
MDA-MB-231	748.0±1.1	183.0±1.2	99.5±1.1

coumarin-6 content was normalized to total cellular protein to calculate nanoparticle uptake in cells.

For confocal microscopy, MA148 cells were plated in 2-chamber Lab-Tek® slides (Thermo Scientific) and allowed to attach overnight. Following incubation with 100 μg/ml of nanoparticles (labeled with coumarin-6) for 1 h at 37°C, cells were washed with DPBS and stained with LysoTracker ® red DND-99 for 30 min at 37°C or Texas red®-X conjugated wheat germ agglutinin for 10 min at 37°C. After three washes with HBSS, cells were fixed with 10% formalin in PBS for 5 min followed by nuclear counterstaining with DAPI (Invitrogen) for 5 min at 37°C. The slide chambers were washed and mounted with a 22×22 mm cover glass using Slowfade® gold (Invitrogen) as the mounting medium. The slides were imaged using a 60X/1.30 numerical aperture oil-immersion objective in an Olympus FluoView FV1000 BX2 upright confocal microscope. Images acquired under green, red, and blue filters were analyzed using FV1000 Viewer software (Olympus Corporation) and ImageJ (NIH).

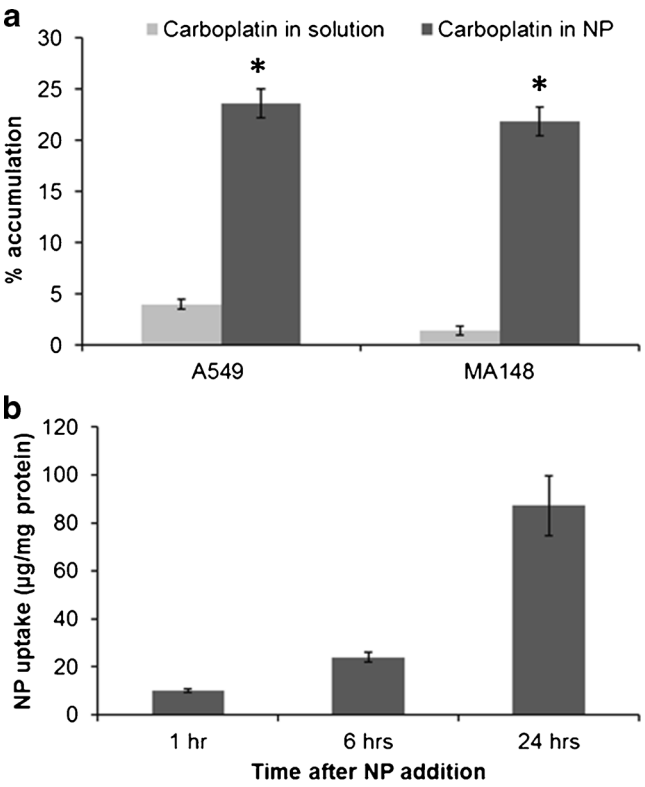

Fig. 4. Enhanced cellular uptake of carboplatin delivered in nanoparticles. **a** Comparison of cellular uptake of free and nanoparticle-encapsulated carboplatin. MA148 and A549 cells were incubated with 1 μg equivalent of carboplatin in solution and nanoparticles for 6 h at 37°C. Following incubation, the cells were washed, lysed, and analyzed for carboplatin content by ICP-MS. Data shown is mean ± SD, $n=3$. *$P<0.01$ vs. carboplatin solution. **b** Nanoparticle uptake in the cells. Control nanoparticles were incubated with MA148 cells for 1, 6, or 24 h. At the end of each time point, the cells were washed, lysed, and the coumarin-6 concentration was quantified to determine nanoparticle levels in the cells. Data shown is mean ± SD, $n=3$

RESULTS

Nanoparticle Characterization

The results from the characterization of carboplatin-loaded PLGA nanoparticles prepared by two different methods are shown in Table I. The physicochemical characteristics of carboplatin nanoparticles were similar to that reported for other PLGA nanoparticles (17). The average hydrodynamic diameter of nanoparticles prepared by the two techniques was comparable and slightly higher than control nanoparticles. Similar appearance and size distribution of nanoparticles prepared by the two methods was also evident from their SEM images (Fig. 1a, b). The polydispersity index of all formulations was less than 0.2, suggesting a narrow size distribution. The zeta potential of all the formulations was negative, which is commonly observed for PLGA nanoparticles without any surface modifications (23). Despite similar particle size and zeta potential, both the loading and the encapsulation efficiency were higher in nanoparticles prepared by Method B than those prepared by Method A. Hence, nanoparticles prepared by Method B were used for all subsequent studies.

The percent release of carboplatin as a function of time is shown in Fig. 2, and the fits to different release kinetic models are summarized in Table II. As evident from the fit data, the overall release profile followed square root-time dependence ('Higuchi pattern'). Interestingly, no initial burst was observed, and near complete release of carboplatin was achieved in 7 days.

Cytotoxicity Studies

The IC_{50} values for free carboplatin in different cell lines were determined as a function of treatment time and concentration. The percent cells surviving for select cell types and days of exposure to carboplatin solution, carboplatin nanoparticles, and controls are given in Fig. 3. The curves were generally fit well by a sigmoidal curve except for MA148 after 1 day, which appeared linear, and the controls, which did not appreciably affect cytotoxicity. In all cases, encapsulation of carboplatin resulted in a significant decrease in the IC_{50}.

The data for the solutions controls in all cell types on days 1, 2, and 3 is shown in Table III. For each cell type, the IC_{50} decreased from day 1 to day 3. As can be seen on day 3, MA148 cells had the lowest IC_{50} followed in order by than NCI-ADR/RES, A549, and MDA-MB-231 cells. Encapsulation in nanoparticles dramatically improved the cytotoxicity of carboplatin and reduced the IC_{50} in all the cell lines. In MA148 cells, the IC_{50} for carboplatin in nanoparticles was 294 ng/ml after 1 day and 110 ng/ml after 2 days of treatment, which were 280- and 255-fold improvements compared to corresponding free carboplatin IC_{50}s (83.7 and 27.9 μg/ml,

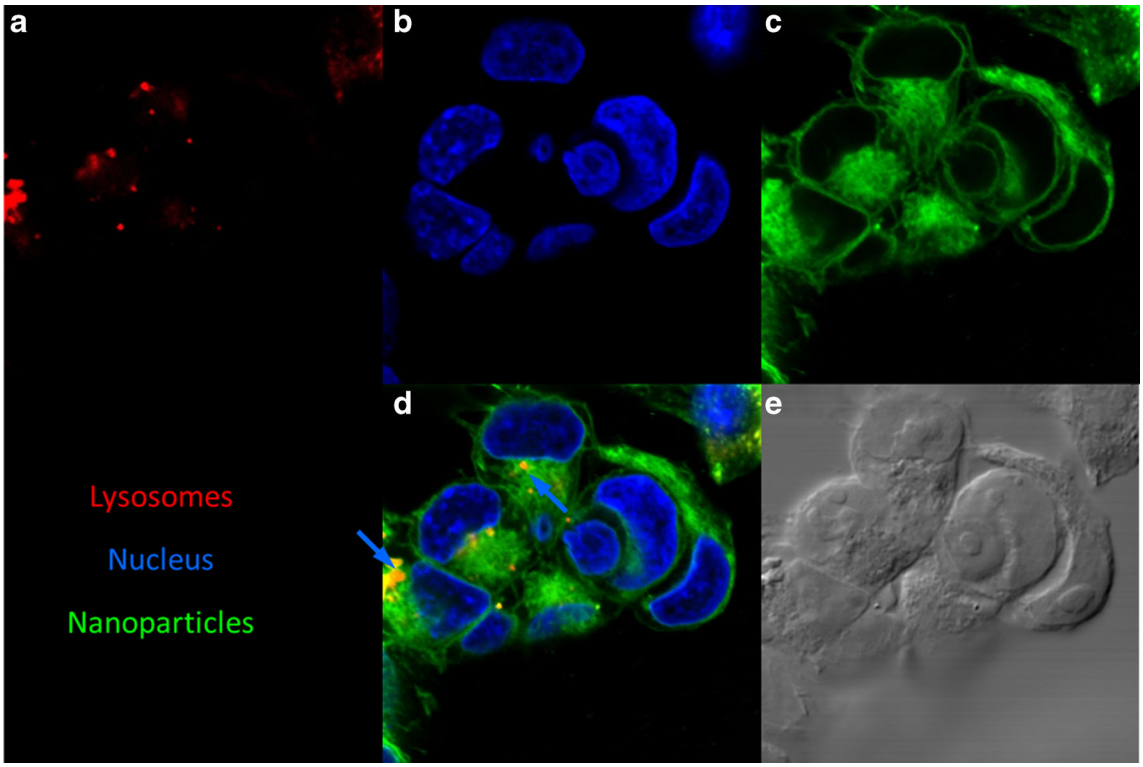

Fig. 5. Intracellular distribution of PLGA nanoparticles. Confocal microscopic images of MA148 cells incubated with coumarin-6 labeled nanoparticles (*green*). Lysosomes were stained with LysoTracker red® (*red*) and nucleus with DAPI (*blue*). Representative images showing the location of **a** lysosomes, **b** nucleus, **c** nanoparticles, and **d** their colocalization. The merged image shows nanoparticles in lysosomes (*blue arrow*) and in the cytoplasm. **e** DIC image of the cells are also shown

respectively) (Fig. 3a, b). Control nanoparticles without carboplatin were not cytotoxic to the cells at the concentrations tested (Fig. 3f).

Intracellular Accumulation of Carboplatin

To explore the mechanism of enhanced cytotoxic efficacy of carboplatin nanoparticles, the cellular accumulation of carboplatin with nanoparticle and solution exposures was quantified 6 h after treatment. ICP-MS analysis revealed that the intracellular platinum concentrations were 6- and 15-fold higher in A549 and MA148 cells, respectively, in nanoparticle treatment groups relative to the solution treatment groups (Fig. 4a). Based on an analysis of the intracellular concentration and administered mass, less than 5% of the carboplatin accumulated within the cells when delivered as solution, whereas more than 20% of the drug was recovered in the cells when introduced in nanoparticles. While the uptake of carboplatin was determined at 6 h, our studies show that there was continued uptake of nanoparticles for at least up to 24 h in MA148 cells (Fig. 4b). This suggests the potential for even further improvement in intracellular delivery of carboplatin with longer incubation times.

Nanoparticle Uptake inside the Cells

The time dependence of uptake as well as the cellular distribution of coumarin-6 labeled PLGA nanoparticles in MA148 cells was assessed by confocal microscopy. Cellular uptake of nanoparticles could be quantitated at 1 h of incubation in MA148 cells (Fig. 4b). Intracellular accumulation of nanoparticles was found to increase as a function of incubation time. Confocal microscopic images revealed the presence of nanoparticles in the lysosomes (colocalization with LysoTracker red) (Fig. 5), on cell surfaces (colocalization with wheat germ agglutinin) (Fig. 6), in the cytoplasm (Figs. 4 and 5), and in the nuclei (colocalization with DAPI) (Fig. 6). Unlike free carboplatin, which does not penetrate well into cells (13), carboplatin-loaded nanoparticles were taken up by the cells efficiently. Furthermore, while a fraction of the nanoparticle-associated fluorescence was localized in the acidic vesicles within the cells (lysosomes and/or endosomes), a significant fraction was found outside of these vesicles and distributed throughout the cells.

DISCUSSION

Polymeric nanoparticles, such as those fabricated from PLGA, are highly suited for the delivery of hydrophobic small molecules and hydrophilic macromolecules. However, they do not efficiently encapsulate hydrophilic small molecules. Despite this challenge, PLGA nanoparticles have been used previously for the delivery of various hydrophilic drugs (24). For drugs like carboplatin, which have poor solubility in organic solvents and limited aqueous solubility, one approach to improve drug loading is to use a suspension of the drug in the inner aqueous phase (25). Alternatively, drug loading can be improved through rapid (<30 min) removal of chloroform rather than through overnight stirring as is usually done for PLGA nanoparticles (26, 27). The latter approach was used to

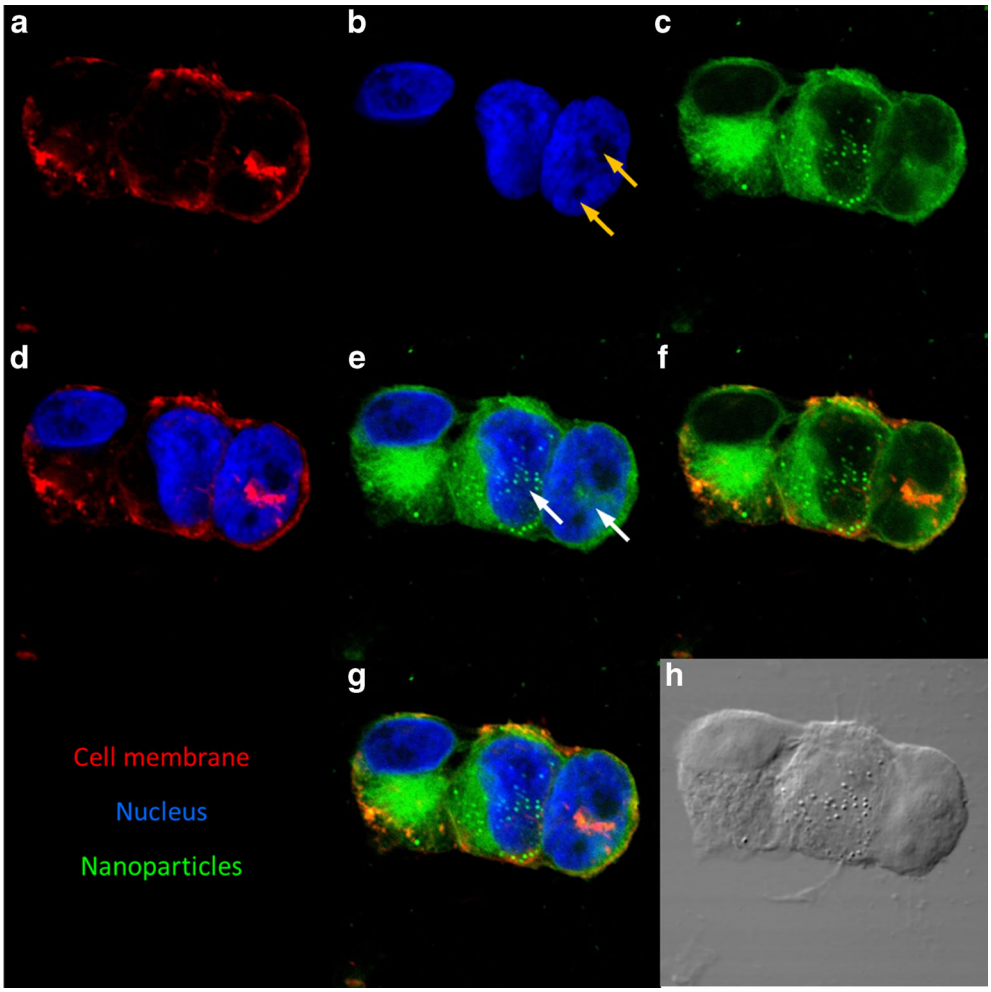

Fig. 6. PLGA nanoparticles can enter the nucleus of dividing cells. Confocal microscopic images of MA148 cells treated with coumarin-6 labeled nanoparticles (*green*). Cell membrane was stained with Texas red®-X conjugated wheat germ agglutinin (*red*) and nucleus was stained with DAPI (*blue*). Representative images showing the individual staining of **a** cell membrane, **b** nucleus, **c** nanoparticles, merged image of **d** cell membrane and nucleus, **e** nanoparticles and nucleus, **f** nanoparticles and cell membrane, and **g** their colocalization. Presence of two nucleoli (*yellow arrows*) suggests cell division. *White arrows* indicate the presence of nanoparticles in the nuclear compartment of the cells. Absence of nanoparticles in nondividing cells (left most cell) and their presence in dividing cells indicate the possibility of nanoparticle entry into the nucleus of the rapidly dividing cells **h** Differential interference contrast (DIC) image of the cells

load carboplatin in PLGA nanoparticles. While the loading and encapsulation efficiency was low compared to that observed for hydrophobic drugs such as paclitaxel, it was on par with the encapsulation efficiency that has been reported for cisplatin prodrugs in PLGA-PEG nanoparticles. This latter system was prepared by nanoprecipitation technique (28).

There are two key differences in the nanoparticle preparation methods that could explain the higher loading and encapsulation efficiency achieved with Method B. BSA was used instead of PVA as the primary emulsion stabilizer in Method B. Previous studies (29, 30) have shown that the primary emulsion stability is greatly improved due to interaction of interfacial film of BSA with polyester polymers, resulting in more stable and better-formed particles. Enhanced stability of the primary emulsion could prevent drug loss from the innermost aqueous core and thereby improve drug loading in nanoparticles. The other difference stems from the rate of evaporation of the organic phase from the W/O/W emulsion. Method A involves slow (~18 h) evaporation of chloroform, which allows longer time for the drug in the innermost aqueous core to escape into the continuous phase. In contrast, Method B involves faster (~30 min) removal of chloroform, leading to rapid nanoparticle formation (27). This could potentially limit the loss of drug during particle formation and higher loading of carboplatin in these nanoparticles.

Carboplatin release from nanoparticles was characterized by lack of burst release and a near complete drug release by 7 days. While the overall release profile was best fit to square-root time dependence, the terminal phase (3–7 days) of the release profile could be fit well with both square-root time dependence and zero-order kinetics. PLGA nanoparticles containing hydrophobic drugs often display an initial burst release, which can be attributed to unencapsulated drug residing on the surface of the nanoparticles. However, due to the

hydrophilic nature of carboplatin, the multiple washing steps during the fabrication procedure likely eliminated any unencapsulated carboplatin. This could explain the lack of burst release from these nanoparticles. Also, the presence of suspended (undissolved) drug in the polymer matrix probably contributes to the sustained drug release as noted by others (27). It would appear that the suspended drug provides a reservoir to maintain a constant driving force for diffusion of carboplatin out of nanoparticles. In addition, BSA could act as a diluent and help to achieve a continuous release of the drug.

Encapsulation in PLGA nanoparticles significantly improved the cytotoxicity of carboplatin. As a general trend, the IC_{50} values decreased with time of treatment incubation. This is expected for carboplatin, which forms intrastrand adducts with DNA, and thereby alters the conformation of DNA and its replication potential (31). Thus, while the untreated cells proliferate and multiply normally, carboplatin treatment results in cell stasis, eventually leading to cell death. This dual effect on cell proliferation manifests itself as lowering of the IC_{50} in the treatment groups over time (32). The IC_{50} values for the free carboplatin were in the same range as that previously reported (33, 34). The IC_{50} values differed among the cell lines used in this study. Encapsulation in nanoparticles not only resulted in improved therapeutic efficacy of carboplatin, but also increased the spectrum of tumor cells that can be effectively treated with carboplatin.

There are numerous reports on the mechanism of resistance of cancer cells to soluble platinum drugs (6). Carboplatin is highly polar and enters cells relatively slowly in comparison to other hydrophobic drugs. Additionally, the uptake of soluble platinum compounds is influenced by factors such as pH, ion concentration, and the presence of reducing agents along with the presence of transporters or gated channels (35). In contrast, polymeric nanoparticles are taken up by cells by endocytosis (36), which is an active process having a rapid onset (37) and thereby resulting in enhanced cellular accumulation of carboplatin. This enhanced cellular uptake potentially translated to higher cytotoxicity of nanoparticle-encapsulated carboplatin (Fig. 6). It is interesting to note that despite releasing only 60–70% of the encapsulated drug in 3 days, nanoparticle-encapsulated carboplatin was more effective than the free drug. Previous studies suggest that encapsulation in nanoparticles results in increased availability of the drug at the site of action, and this could potentially contribute to the enhanced effectiveness of nanoparticle formulation (38).

Confocal images of cells treated with carboplatin nanoparticles confirmed nanoparticle uptake and intracellular distribution after 1 h of incubation. Colocalization of nanoparticles within the acidic vesicles suggests that nanoparticles enter the cells by endocytosis, as has been reported before (19). Similar to that observed in previous studies, our studies also show that PLGA nanoparticles can escape the endolysosomal compartment and enter the cytoplasm (19). Nanoparticles in the cytoplasm can release their cargo directly inside the cells, which can overcome the low cellular uptake observed for hydrophilic drugs. Our studies further suggest that improved efficacy of nanoparticles could also be due to nuclear uptake of nanoparticles and direct delivery of carboplatin to its principal site of action within the tumor cell. The nuclear pores of the cells are too small (~10 nm) to allow nanoparticles to enter the intact nucleus (39). However, during cell division, the nuclear membrane dissolves, and this presents an opportunity for nanoparticles to enter the nuclear space. The presence of two nucleoli (yellow arrows, Fig. 6b) indicating cell division (40), and the presence of nanoparticles inside the nucleus of the dividing cells (white arrows, Fig. 6e) provides support for this argument. Absence of nanoparticles in the nucleus of nondividing cells (left cell with intact nucleus) further corroborates this argument. However, additional quantitative studies are needed to confirm improved nuclear delivery of carboplatin with PLGA nanoparticles.

Our studies demonstrate that nanoparticle encapsulation of hydrophilic drugs like carboplatin can significantly improve their therapeutic effect. While PLGA is FDA approved and has been shown to be safe, other nanoparticle systems can also be employed for hydrophilic drugs (21, 41, 42). Additionally, co-delivery of other cytotoxic drugs along with carboplatin

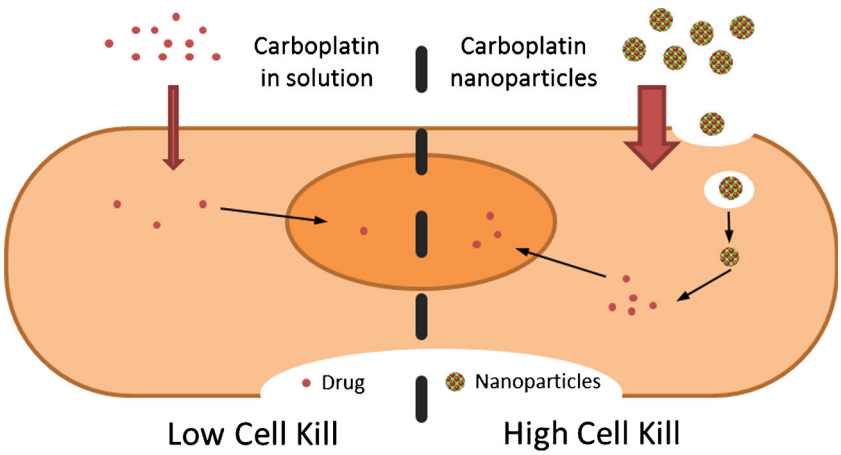

Fig. 7. Mechanism of improved cell kill by nanoparticle encapsulated carboplatin. Free carboplatin exhibits low cellular accumulation due to slow and inefficient uptake by the cells. Nanoparticle encapsulation increases carboplatin uptake and hence improves its intracellular delivery. Enhanced cellular uptake in turn translates to higher cell kill by nanoparticle-encapsulated carboplatin

and surface modification of nanoparticles to incorporate targeting ligands could result in further enhanced therapeutic efficacy (18). In addition to improving the carboplatin loading, our future studies will evaluate the *in vivo* anticancer efficacy of carboplatin-loaded nanoparticles.

CONCLUSIONS

Despite its hydrophilic nature, carboplatin was successfully loaded into PLGA nanoparticles. The release of carboplatin was sustained over 7 days, with no initial burst. Significantly, lower IC_{50} values in four different cancer cell lines were observed with carboplatin nanoparticles in comparison to solution exposures. This greater cytotoxicity was associated with a more rapid entry of nanoparticles, higher intracellular delivery of drug, and perhaps most significantly, greater distribution within the cell nucleus, the site of action of carboplatin (Fig. 7). Given the favorable nanoparticle, physical-chemical properties and enhanced efficacy in a safe delivery system, carboplatin-loaded PLGA nanoparticles, may prove to be a promising approach to improved cancer chemotherapy.

ACKNOWLEDGMENTS

We thank the University Imaging Centers at the University of Minnesota for assistance with confocal microscopy. Parts of this work were carried out in the Characterization Facility, University of Minnesota, which receives partial support from NSF through the MRSEC program. We also thank the Dr. Rick Knurr, Geochemical Lab in the Department of Earth Sciences at the University of Minnesota for ICP-MS analysis.

REFERENCES

1. Helm CW, States JC. Enhancing the efficacy of cisplatin in ovarian cancer treatment—could arsenic have a role. J Ovarian Res. 2009;2:2.
2. Mutter R, Lu B, Carbone DP, Csiki I, Moretti L, Johnson DH, *et al.* A phase II study of celecoxib in combination with paclitaxel, carboplatin, and radiotherapy for patients with inoperable stage IIIA/B non-small cell lung cancer. Clin Cancer Res Off J Am Assoc Cancer Res. 2009;15(6):2158–65.
3. Aisner J, Sinibaldi V, Eisenberger M. Carboplatin in the treatment of squamous cell head and neck cancers. Semin Oncol. 1992;19(1 Suppl 2):60–5.
4. Möbus V, Wandt H, Frickhofen N, Bengala C, Champion K, Kimmig R, *et al.* Phase III trial of high-dose sequential chemotherapy with peripheral blood stem cell support compared with standard dose chemotherapy for first-line treatment of advanced ovarian cancer: Intergroup trial of the AGO-Ovar/AIO and EBMT. J Clin Oncol. 2007;25(27):4187–93.
5. Jakobsen A, Bertelsen K, Andersen JE, Havsteen H, Jakobsen P, Moeller KA, *et al.* Dose-effect study of carboplatin in ovarian cancer: a Danish Ovarian Cancer Group study. J Clin Oncol. 1997;15(1):193–8.
6. Stewart DJ. Mechanisms of resistance to cisplatin and carboplatin. Crit Rev Oncol Hematol. 2007;63(1):12–31.
7. Colombo N, Guthrie D, Chiari S, Parmar M, Qian W, Swart AM, *et al.* International Collaborative Ovarian Neoplasm trial 1: a randomized trial of adjuvant chemotherapy in women with early-stage ovarian cancer. J Natl Cancer Inst. 2003;95(2):125–32.
8. Rademaker-Lakhai JM, Terret C, Howell SB, Baud CM, De Boer RF, Pluim D, *et al.* A Phase I and pharmacological study of the platinum polymer AP5280 given as an intravenous infusion once every 3 weeks in patients with solid tumors. Clin Cancer Res Off J Am Assoc Cancer Res. 2004;10(10):3386–95.
9. Raynaud FI, Boxall FE, Goddard PM, Valenti M, Jones M, Murrer BA, *et al.* cis-Amminedichloro(2-methylpyridine) platinum(II) (AMD473), a novel sterically hindered platinum complex: in vivo activity, toxicology, and pharmacokinetics in mice. Clin Cancer Res Off J Am Assoc Cancer Res. 1997;3(11):2063–74.
10. Raymond E, Faivre S, Chaney S, Woynarowski J, Cvitkovic E. Cellular and molecular pharmacology of oxaliplatin. Mol Cancer Ther. 2002;1(3):227–35.
11. Sengupta P, Basu S, Soni S, Pandey A, Roy B, Oh MS, *et al.* Cholesterol-tethered platinum II-based supramolecular nanoparticle increases antitumor efficacy and reduces nephrotoxicity. Proc Natl Acad Sci U S A. 2012;109(28):11294–9.
12. Kelland L. The resurgence of platinum-based cancer chemotherapy. Nat Rev Cancer. 2007;7(8):573–84.
13. Hamelers IHL, van Loenen E, Staffhorst RWHM, de Kruijff B, de Kroon AIPM. Carboplatin nanocapsules: a highly cytotoxic, phospholipid-based formulation of carboplatin. Mol Cancer Ther. 2006;5(8):2007–12.
14. Chaudhury A, Das S, Bunte RM, Chiu GN. Potent therapeutic activity of folate receptor-targeted liposomal carboplatin in the localized treatment of intraperitoneally grown human ovarian tumor xenograft. Int J Nanomedicine. 2012;7:739–51.
15. Liu D, He C, Wang AZ, Lin W. Application of liposomal technologies for delivery of platinum analogs in oncology. Int J Nanomedicine. 2013;8:3309–19.
16. Prabha S, Sharma B, Labhasetwar V. Inhibition of tumor angiogenesis and growth by nanoparticle-mediated p53 gene therapy in mice. Cancer Gene Ther. 2012;19(8):530–7.
17. Patil YB, Swaminathan SK, Sadhukha T, Ma L, Panyam J. The use of nanoparticle-mediated targeted gene silencing and drug delivery to overcome tumor drug resistance. Biomaterials. 2010;31(2):358–65.
18. Patil Y, Sadhukha T, Ma L, Panyam J. Nanoparticle-mediated simultaneous and targeted delivery of paclitaxel and tariquidar overcomes tumor drug resistance. J Control Release. 2009;136(1):21–9.
19. Vasir JK, Labhasetwar V. Biodegradable nanoparticles for cytosolic delivery of therapeutics. Adv Drug Deliv Rev. 2007;59(8):718–28.
20. Mittal A, Chitkara D, Kumar N. HPLC method for the determination of carboplatin and paclitaxel with cremophorEL in an amphiphilic polymer matrix. J Chromatogr B Anal Technol Biomed Life Sci. 2007;855(2):211–9.
21. Nanjwade BK, Singh J, Parikh KA, Manvi FV. Preparation and evaluation of carboplatin biodegradable polymeric nanoparticles. Int J Pharm. 2010;385(1–2):176–80.
22. Qaddoumi MG, Ueda H, Yang J, Davda J, Labhasetwar V, Lee VH. The characteristics and mechanisms of uptake of PLGA nanoparticles in rabbit conjunctival epithelial cell layers. Pharm Res. 2004;21(4):641–8.
23. Prabha S, Labhasetwar V. Critical determinants in PLGA/PLA nanoparticle-mediated gene expression. Pharm Res. 2004;21(2):354–64.
24. Park J, Fong PM, Lu J, Russell KS, Booth CJ, Saltzman WM, *et al.* PEGylated PLGA nanoparticles for the improved delivery of doxorubicin. Nanomedicine Nanotechnol Biol Med. 2009;5(4):410–8.
25. Jacobson GB, Shinde R, Contag CH, Zare RN. Sustained release of drugs dispersed in polymer nanoparticles. Angew Chem. 2008;47(41):7880–2.
26. Shahani K, Swaminathan SK, Freeman D, Blum A, Ma L, Panyam J. Injectable sustained release microparticles of curcumin: a new concept for cancer chemoprevention. Cancer Res. 2010;70(11):4443–52.
27. Shahani K, Panyam J. Highly loaded, sustained-release microparticles of curcumin for chemoprevention. J Pharm Sci. 2011;100(7):2599–609.
28. Graf N, Bielenberg DR, Kolishetti N, Muus C, Banyard J, Farokhzad OC, *et al.* alpha(V)beta(3) integrin-targeted PLGA-PEG nanoparticles for enhanced anti-tumor efficacy of a Pt(IV) prodrug. ACS Nano. 2012;6(5):4530–9.

29. Nihant N, Schugens C, Grandfils C, Jerome R, Teyssie P. Polylactide microparticles prepared by double emulsion/evaporation technique. I. Effect of primary emulsion stability. Pharm Res. 1994;11(10):1479–84.
30. Nihant N, Schugens C, Grandfils C, Jerome R, Teyssie P. Polylactide microparticles prepared by double emulsion-evaporation: II. Effect of the poly (Lactide-co-Glycolide) composition on the stability of the primary and secondary emulsions. J Colloid Interface Sci. 1995;173(1):55–65.
31. Go RS, Adjei AA. Review of the comparative pharmacology and clinical activity of cisplatin and carboplatin. J Clin Oncol. 1999;17(1):409–22.
32. Baumann KH, Kim H, Rinke J, Plaum T, Wagner U, Reinartz S. Effects of alvocidib and carboplatin on ovarian cancer cells in vitro. Exp Oncol. 2013;35(3):168–73.
33. Samanta D, Kaufman J, Carbone DP, Datta PK. Long-term smoking mediated down-regulation of Smad3 induces resistance to carboplatin in non-small cell lung cancer. Neoplasia. 2012;14(7):644–55.
34. Wild R, Dings RP, Subramanian I, Ramakrishnan S. Carboplatin selectively induces the VEGF stress response in endothelial cells: Potentiation of antitumor activity by combination treatment with antibody to VEGF. Int J Cancer. 2004;110(3):343–51.
35. Gately DP, Howell SB. Cellular accumulation of the anticancer agent cisplatin: a review. Br J Cancer. 1993;67(6):1171–6.
36. Sahay G, Alakhova DY, Kabanov AV. Endocytosis of nanomedicines. J Control Release Off J Control Release Soc. 2010;145(3):182–95.
37. Davda J, Labhasetwar V. Characterization of nanoparticle uptake by endothelial cells. Int J Pharm. 2002;233(1–2):51–9.
38. Panyam J, Labhasetwar V. Sustained cytoplasmic delivery of drugs with intracellular receptors using biodegradable nanoparticles. Mol Pharm. 2004;1(1):77–84.
39. Pante N, Kann M. Nuclear pore complex is able to transport macromolecules with diameters of about 39 nm. Mol Biol Cell. 2002;13(2):425–34.
40. Tomaso MVD, Liddle P, Lafon-Hughes L, Reyes-Ábalos AL, Folle G. Chromatin Damage Patterns Shift According to Eu/Heterochromatin Replication 2013 2013-02-20.
41. Kang SJ, Durairaj C, Kompella UB, O'Brien JM, Grossniklaus HE. SUbconjunctival nanoparticle carboplatin in the treatment of murine retinoblastoma. Arch Ophthalmol. 2009;127(8):1043–7.
42. Oberoi HS, Laquer FC, Marky LA, Kabanov AV, Bronich TK. Core cross-linked block ionomer micelles as pH-responsive carriers for cis-diamminedichloroplatinum(II). J Control Release. 2011;153(1):64–72.